

## NEW MASS-LOSS MEASUREMENTS FROM ASTROSPHERIC $\text{Ly}\alpha$ ABSORPTION

B. E. WOOD,<sup>1</sup> H.-R. MÜLLER,<sup>2,3</sup> G. P. ZANK,<sup>3</sup> J. L. LINSKY,<sup>1</sup> AND S. REDFIELD<sup>4</sup>

Received 2005 April 26; accepted 2005 June 15; published 2005 July 11

### ABSTRACT

Measurements of stellar mass-loss rates are used to assess how wind strength varies with coronal activity and age for solar-like stars. Mass loss generally increases with activity, but we find evidence that winds suddenly weaken at a certain activity threshold. Very active stars are often observed to have polar starspots, and we speculate that the magnetic field geometry associated with these spots may be inhibiting the winds. Our inferred mass-loss/age relation represents an empirical estimate of the history of the solar wind. This result is important for planetary studies as well as solar/stellar astronomy, since solar wind erosion may have played an important role in the evolution of planetary atmospheres.

*Subject headings:* circumstellar matter — stars: winds, outflows — ultraviolet: stars

### 1. INTRODUCTION

The weak winds generated by solar-like stars are normally undetectable to remote sensing. However, these winds ultimately collide with the interstellar medium (ISM) surrounding the star, and if the surrounding ISM is at least partially neutral this collision yields a population of hot hydrogen atoms that produces a detectable absorption signature in spectra of the stellar  $\text{Ly}\alpha$  line. Spectra obtained by the *Hubble Space Telescope* (*HST*) have provided detections of this absorption from hydrogen in the outer regions of our own heliosphere as well as many detections of absorption from the “astrospheres” surrounding the observed stars (e.g., Linsky & Wood 1996; Wood et al. 1996, 2000).

The detection of astrospheres not only represents the first clear detection of solar-like winds from other stars but it also allows the first estimates of mass-loss rates from these stars, since the amount of absorption is correlated with the strength of the wind. These measurements have been used to investigate how mass loss varies with age and coronal activity for solar-like stars. Initial results suggest that younger stars with more active coronae have stronger winds (Wood et al. 2002, hereafter Paper I), implying that the solar wind was stronger in the past. We have recently analyzed all appropriate  $\text{Ly}\alpha$  spectra in the *HST* archive to search for new astrospheric detections (Wood et al. 2005, hereafter Paper II). In this Letter, we estimate mass-loss rates for the seven new astrospheric absorption detections resulting from this archival  $\text{Ly}\alpha$  work, and we reassess what the astrospheric absorption is telling us about how winds correlate with stellar age and activity.

### 2. NEW MASS-LOSS MEASUREMENTS

Table 1 lists both the new and old mass-loss measurements from astrospheric absorption detections. In cases where members of a binary system are close enough to be within the same astrosphere (e.g.,  $\alpha$  Cen), the spectral types of both stars are given, since the measured mass-loss rate will be the combined

mass loss from both stars. Likewise, the stellar surface area listed in the table will in those cases be the binary’s combined surface area. The surface areas are computed from stellar radii listed in Paper II. The coronal X-ray luminosities listed in the second to last column of Table 1 (in units of  $\text{ergs s}^{-1}$ ) are *ROSAT* All-Sky Survey measurements (see Paper II).

In order to measure a mass-loss rate from the observed astrospheric absorption, it is necessary to know the ISM wind velocity seen by the star ( $V_{\text{ISM}}$ ) and the orientation of the astrosphere relative to our line of sight ( $\theta$ ), which are both listed in Table 1. The orientation angle,  $\theta$ , is the angle between the upwind direction of the ISM flow seen by the star and our line of sight to the star. The  $V_{\text{ISM}}$  and  $\theta$  values in Table 1 are computed from the known proper motions and radial velocities of the observed stars, and by assuming that the local interstellar cloud flow vector of Lallement & Bertin (1992) applies for the ISM surrounding all observed stars. For a few stars known to be in directions where the slightly different G cloud vector of Lallement & Bertin (1992) is more applicable ( $\alpha$  Cen, 36 Oph, 70 Oph), we use this vector instead.

The mass-loss measurement process is described in detail in Paper I and in Wood (2004). Briefly, hydrodynamic models of the astrospheres, constrained by the  $V_{\text{ISM}}$  values in Table 1, are computed using a four-fluid code developed to model the heliosphere and reproduce the observed heliospheric  $\text{Ly}\alpha$  absorption (Zank et al. 1996; Wood et al. 2000). Models with different mass-loss rates are computed by varying the stellar wind density. Predicted astrospheric  $\text{Ly}\alpha$  absorption can be computed from these models for the observed line of sight defined by the  $\theta$  value in Table 1. Paper I and Wood (2004) discuss systematic errors in detail, such as uncertainties in ISM properties, wind velocities, and wind variability, concluding that the derived mass-loss rates have uncertainties of order a factor of 2 due to these systematics. Uncertainties of this size are consistent with the results of Izmodenov et al. (2002) and Florinski et al. (2004), who have studied how heliospheric  $\text{Ly}\alpha$  absorption should change with variations in ISM parameters such as the ionization fraction and magnetic field strength. The assumption of the same  $400 \text{ km s}^{-1}$  wind speed in all astrospheric models (akin to solar low-speed streams) is another major source of uncertainty, its justification being that one might expect similar wind speeds from stars with similar spectral types and surface escape speeds (Wood 2004).

Figure 1 compares the observed astrospheric absorption with model predictions. Mass-loss rates are quoted relative to the

<sup>1</sup> JILA, University of Colorado and NIST, 440 UCB, Boulder, CO 80309-0440; woodb@origins.colorado.edu, jlinsky@jila.colorado.edu.

<sup>2</sup> Department of Physics and Astronomy, Dartmouth College, 6127 Wilder Laboratory, Hanover, NH 03755-3528; hans.mueller@dartmouth.edu.

<sup>3</sup> Institute of Geophysics and Planetary Physics, University of California at Riverside, 1432 Geology, Riverside, CA 92521; zank@ucra1.ucr.edu.

<sup>4</sup> Harlan J. Smith Postdoctoral Fellow, McDonald Observatory, University of Texas at Austin, 1 University Station, C1402, Austin, TX 78712-0259; sreedfield@astro.as.utexas.edu.

TABLE 1  
MASS-LOSS MEASUREMENTS FROM ASTROSPHERIC DETECTIONS

Star	Spectral Type	$d$ (pc)	$V_{\text{ISM}}$ (km s $^{-1}$ )	$\theta$ (deg)	$\dot{M}$ ( $M_{\odot}$ )	$\log L_{\text{x}}$	Surface Area ( $A_{\odot}$ )
Previous Analyses							
Proxima Cen .....	M5.5 V	1.30	25	79	<0.2	27.22	0.023
$\alpha$ Cen .....	G2 V + K0 V	1.35	25	79	2	27.70	2.22
$\epsilon$ Eri .....	K1 V	3.22	27	76	30	28.32	0.61
61 Cyg A .....	K5 V	3.48	86	46	0.5	27.45	0.46
$\epsilon$ Ind .....	K5 V	3.63	68	64	0.5	27.39	0.56
36 Oph .....	K1 V + K1 V	5.99	40	134	15	28.34	0.88
$\lambda$ And .....	G8 IV–III + M V	25.8	53	89	5	30.82	54.8
New Analyses							
EV Lac .....	M3.5 V	5.05	45	84	1	28.99	0.123
70 Oph .....	K0 V + K5 V	5.09	37	120	100	28.49	1.32
$\xi$ Boo .....	G8 V + K4 V	6.70	32	131	5	28.90	1.00
61 Vir .....	G5 V	8.53	51	98	0.3	26.87	1.00
$\delta$ Eri .....	K0 IV	9.04	37	41	4	27.05	6.66
HD 128987 .....	G6 V	23.6	8	79	?	28.60	0.71
DK UMa .....	G4 III–IV	32.4	43	32	0.15	30.36	19.4

solar value of  $\dot{M}_{\odot} \approx 2 \times 10^{-14} M_{\odot} \text{ yr}^{-1}$ . Table 1 lists the mass-loss rates that yield the best fits to the data. When evaluating how well a model fits the data, it is more important that the model fits well near the base of the H I absorption than elsewhere, since discrepancies farther from the core of the absorption can often be resolved simply by altering the assumed stellar emission profile. Thus, the  $\dot{M} = 1 M_{\odot}$  model for EV Lac is deemed a better fit than the  $\dot{M} = 2 M_{\odot}$  model, for example.

The astrospheric models that yield the best fits to the data

are illustrated in Figure 2. Most of the absorption we observe comes from the “hydrogen wall” region in between the astropause and the stellar bow shock, which is colored a purplish-red in Figure 2. Because it will generally take more than a decade for wind material to reach these distances (e.g., Zank et al. 1996), mass-loss rate measurements from astrospheric absorption will typically be indicative of the average mass loss over decadal timescales, except for the most compact astrospheres ( $\epsilon$  Ind, 61 Cyg A, and DK UMa), and the astrospheric absorption will not vary on shorter timescales such as those

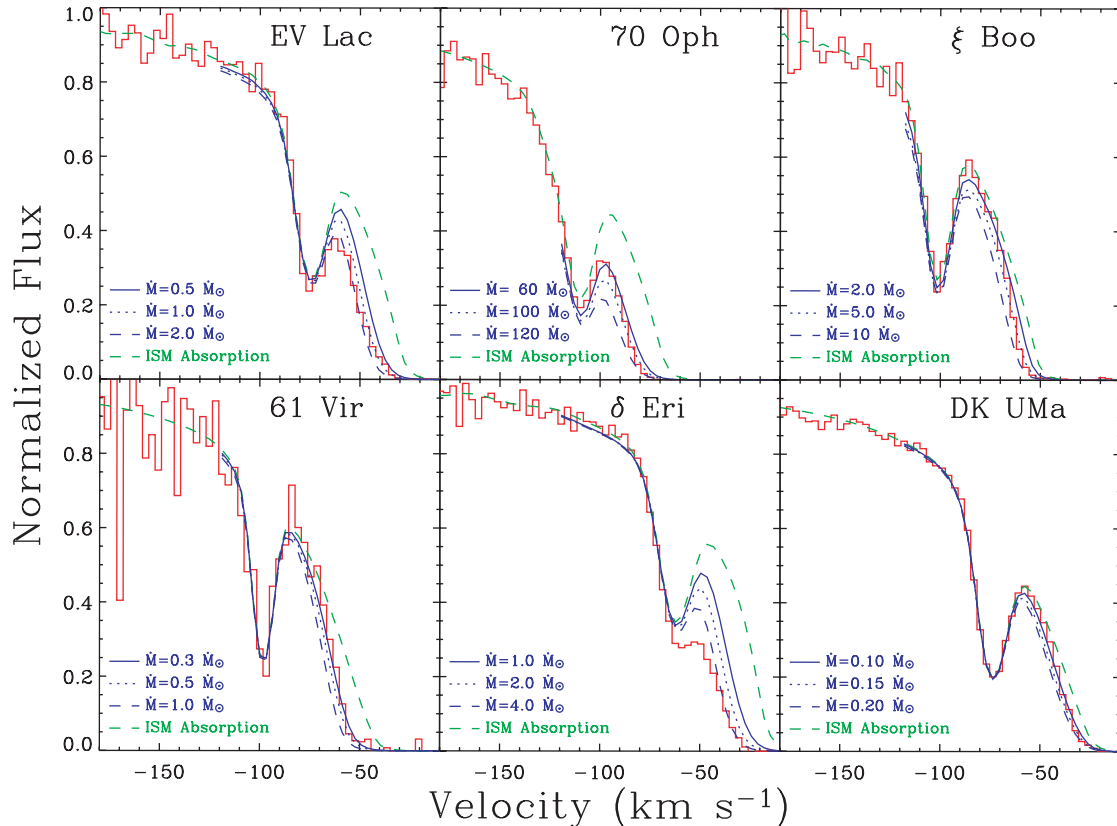


FIG. 1.—Blue side of the H I Ly $\alpha$  absorption lines for the new astrospheric absorption detections. The green dashed lines show the ISM absorption, and the blue dashed lines show the additional astrospheric absorption predicted by models assuming various mass-loss rates.

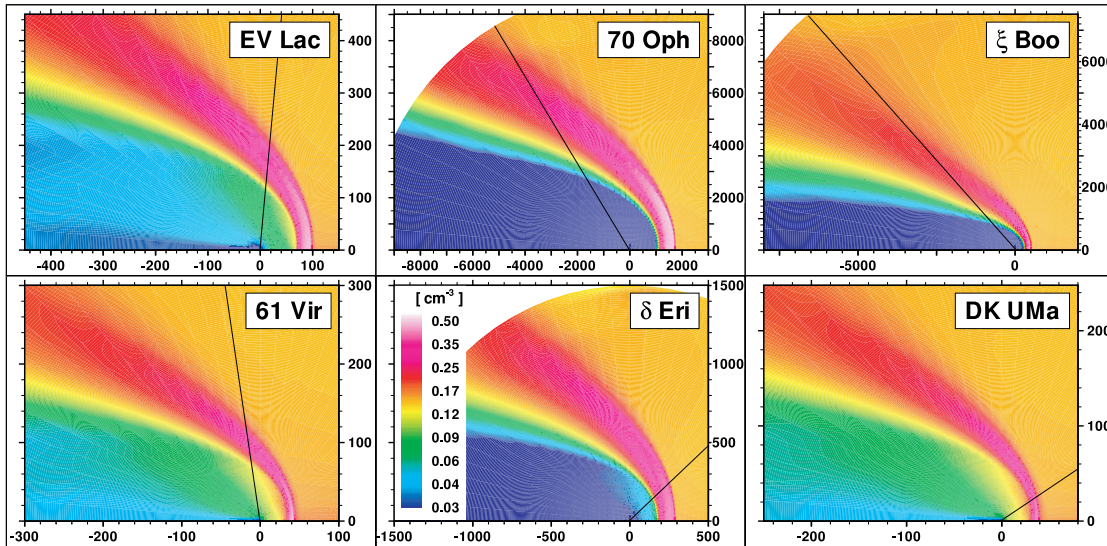


FIG. 2.—Maps of H I density for the astrospheric models that yield the best fits to the data in Fig. 1. The distance scale is in AU. The laminar ISM wind seen by the star comes from the right. Solid lines indicate the observed Sun-star line of sight.

associated with activity cycles. We also note that in cases where the size of the modeled astrosphere indicates that both stars of a binary system are within the same astrosphere ( $\alpha$  Cen, 36 Oph,  $\lambda$  And, 70 Oph, and  $\xi$  Boo), there is no way for us to tell how much each star is contributing to the combined binary wind or if the combined wind's ram pressure has been reduced by wind interaction effects.

For one of the new astrospheric detections, HD 128987, we find that the astrospheric models are unable to adequately fit the data regardless of the assumed mass-loss rate, so no mass-loss measurement is listed for this star in Table 1. The primary cause of our difficulties with HD 128987 is its very low ISM speed of  $V_{\text{ISM}} = 8 \text{ km s}^{-1}$ . High ISM velocities yield more heating and deceleration of H I at the stellar bow shock. This results in astrospheric H I that is hot and highly decelerated, meaning that Ly $\alpha$  absorption from this material is broad and shifted away from the ISM absorption. This is why astrospheric absorption is detectable despite being highly blended with the ISM absorption (see Paper II). Thus, it is surprising that astrospheric absorption has been detected for a star with such a

low  $V_{\text{ISM}}$  value, and our astrospheric models have not been able to explain the observed absorption. More work must be done in the future to offer a satisfactory explanation for this unusual case.

In Figure 3a we plot our measured mass-loss rates (per unit surface area) versus X-ray surface fluxes. For solar-like stars, X-ray emission and winds both arise from the hot stellar coronae. Thus, one might expect to see a correlation of some sort between X-ray emission and mass loss. For the main-sequence stars, mass loss appears to increase with activity for  $\log F_x < 8 \times 10^5 \text{ ergs cm}^{-2} \text{ s}^{-1}$ . The power-law relation that we have fitted to the data in Figure 3a,  $\dot{M} \propto F_x^{1.34 \pm 0.18}$ , is consistent with that reported in Paper I. However, the new  $\xi$  Boo data point suggests that the relation does not extend to high activity levels.

In Paper I, we suggested that the apparent inconsistency of Proxima Cen (M5.5 V) and  $\lambda$  And (G8 IV–III + M V) with the mass-loss/activity relation was due to these stars being less solar-like than the GK main-sequence stars, but the new low mass-loss measurement for  $\xi$  Boo, which is a G8 V + K4 V binary, suggests that the relation simply does not extend to

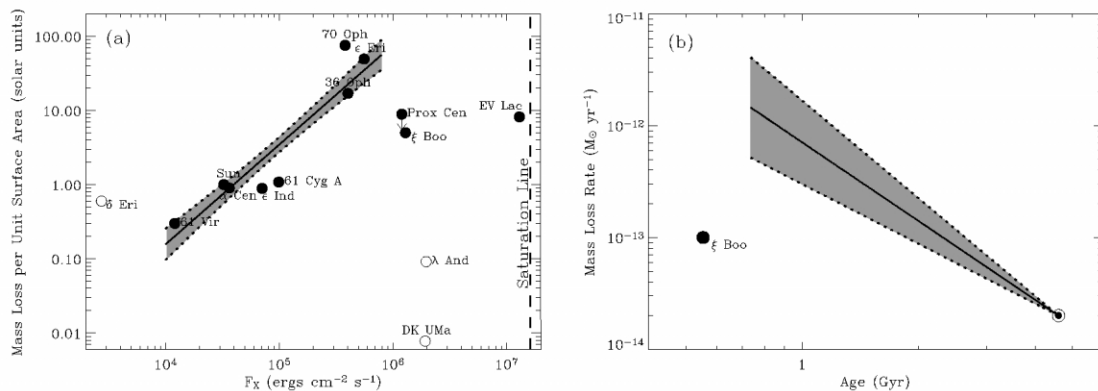


FIG. 3.—(a) Mass-loss rates per unit surface area plotted vs. stellar X-ray surface fluxes. The filled circles are for main-sequence stars, while the open circles are for evolved stars. For main-sequence stars with  $\log F_x < 8 \times 10^5 \text{ ergs cm}^{-2} \text{ s}^{-1}$ , mass loss increases with X-ray flux, and we have fitted a power law to these data points. Uncertainties in this relation are estimated as described in Paper I. (b) Mass-loss history of the Sun inferred from the power-law relation in (a). The truncation of the relation in (a) means that the mass-loss/age relation is truncated as well. The low mass-loss measurement for  $\xi$  Boo suggests that the wind suddenly weakens at  $t \approx 0.7 \text{ Gyr}$  as one goes back in time.

high activity levels for *any* type of star. Therefore, the power law in Figure 3a has been truncated at  $\log F_x = 8 \times 10^5 \text{ ergs cm}^{-2} \text{ s}^{-1}$ . All five of the higher activity stars have mass-loss rates much lower than the power law would suggest. The three evolved stars in Figure 3a ( $\delta$  Eri,  $\lambda$  And, and DK UMa) do not seem to have mass-loss rates consistent with those of the main-sequence stars. The very active coronae of  $\lambda$  And and DK UMa produce surprisingly weak winds, although it should be noted that both of these astrophysical detections are flagged as being questionable in Paper II. Clearly more mass-loss measurements would be helpful to better define the mass-loss/activity relation of cool main-sequence stars, especially at high activity levels where more measurements of truly solar-like G and K dwarf stars are necessary to see exactly what is happening to solar-like winds at high coronal activity. Additional measurements are also required to determine whether or not G, K, and M dwarfs all show the same mass-loss/activity relations. Currently, our sample is simply not large enough to precisely address these questions.

Why does the mass-loss/activity relation apparently change its character at  $\log F_x \approx 8 \times 10^5 \text{ ergs cm}^{-2} \text{ s}^{-1}$ ? One possible explanation concerns the appearance of polar spots for very active stars. Low-activity stars presumably have solar-like star-spot patterns, where the spots are always confined to low latitudes. However, for very active stars, not only are spots detected at high latitudes but a majority of these stars show evidence of large polar spots (Strassmeier 2002). The appearance of high-latitude and polar spots represents a fundamental change in the stellar magnetic geometry (Schrijver & Title 2001), and it is possible that this dramatic change in the magnetic field structure could affect the winds emanating from these stars. We hypothesize that stars with polar spots might have a magnetic field with a strong dipolar component that could envelope the entire star and inhibit stellar outflows, thereby explaining why active stars have weaker winds than the mass-loss/activity relation of less active main-sequence stars would predict. For  $\xi$  Boo A, high-latitude spots of some sort have been detected (Toner & Gray 1988), and Petit et al. (2005) have detected both global dipole and large-scale toroidal field components.

As we did in Paper I, we combine the mass-loss/activity relation in Figure 3a with a known relation between activity

and age,  $F_x \propto t^{-1.74 \pm 0.34}$  (Ayres 1997), to derive an empirical mass-loss evolution law for solar-like stars:  $\dot{M} \propto t^{-2.33 \pm 0.55}$ . Figure 3b shows what this relation suggests for the mass-loss history of the Sun. The truncation of the power-law relation in Figure 3a leads to the mass-loss/age relation in Figure 3b being truncated as well at about  $t = 0.7$  Gyr. Mass-loss rates for very active stars are significantly lower than would be predicted by the mass-loss/activity relation defined by the less active stars, with the  $\xi$  Boo example being particularly relevant since the stars in this binary are easily the most solar-like of those in this high-activity regime. Thus, the location of  $\xi$  Boo is shown in Figure 3b in order to infer what the solar wind might have been like at times earlier than  $t = 0.7$  Gyr.

The history of the solar wind is not only of interest to solar/stellar astronomers but is also important for planetary studies (Ribas et al. 2005). Stellar winds can potentially erode planetary atmospheres, and the strong winds that apparently exist for young stars make it even more likely that winds have a significant impact on planets. Work has begun on how stellar winds might affect the atmospheres of detected extrasolar planets (Griessmeier et al. 2004). In our own solar system, the impact of the solar wind on the atmospheres of Venus and Titan has been explored (Chassefière 1997; Lammer et al. 2000), but the most intriguing case study by far is Mars, since the history of the Martian atmosphere is intimately connected with the history of water and perhaps life on the surface of the planet. Mars lost most its atmosphere early in its history, possibly due to solar wind erosion (e.g., Lammer et al. 2003). This did not happen on Earth, presumably due to the protection from the solar wind provided by the Earth's strong magnetosphere. Unlike Earth, Mars lost its global magnetic field at least 3.9 Gyr ago (Acuña et al. 1999), and this is roughly the period when most of its atmosphere and surface water are believed to have disappeared as well. Interestingly enough, the time when Mars is believed to have lost most of its atmosphere corresponds roughly to the time when Figure 3b suggests that the solar wind abruptly strengthens ( $t \approx 0.7$  Gyr). Perhaps this strengthening of the solar wind, which we have speculated might be connected to the loss of polar spots, played a central role in the dissipation of the Martian atmosphere.

Support for this work was provided by NASA grant NNG05GD69G and grant AR-09957 from STScI.

#### REFERENCES

- Acuña, M. H., et al. 1999, *Science*, 284, 790  
 Ayres, T. R. 1997, *J. Geophys. Res.*, 102, 1641  
 Chassefière, E. 1997, *Icarus*, 126, 229  
 Florinski, V., Pogorelov, N. V., Zank, G. P., Wood, B. E., & Cox, D. P. 2004, *ApJ*, 604, 700  
 Griessmeier, J.-M., et al. 2004, *A&A*, 425, 753  
 Izmodenov, V. V., Wood, B. E., & Lallement, R. 2002, *J. Geophys. Res.*, 107, 1308  
 Lallement, R., & Bertin, P. 1992, *A&A*, 266, 479  
 Lammer, H., Lichtenegger, H. I. M., Kolb, C., Ribas, I., Guinan, E. F., Abart, R., & Bauer, S. J. 2003, *Icarus*, 165, 9  
 Lammer, H., Stumptner, W., Molina-Cuberos, G. J., Bauer, S. J., & Owen, T. 2000, *Planet. Space Sci.*, 48, 529  
 Linsky, J. L., & Wood, B. E. 1996, *ApJ*, 463, 254  
 Petit, P., et al. 2005, *MNRAS*, in press  
 Ribas, I., Guinan, E. F., Güdel, M., & Audard, M. 2005, *ApJ*, 622, 680  
 Schrijver, C. J., & Title, A. M. 2001, *ApJ*, 551, 1099  
 Strassmeier, K. G. 2002, *Astron. Nachr.*, 323, 309  
 Toner, C. G., & Gray, D. F. 1988, *ApJ*, 334, 1008  
 Wood, B. E. 2004, *Living Rev. Sol. Phys.*, 1, 2  
 Wood, B. E., Alexander, W. R., & Linsky, J. L. 1996, *ApJ*, 470, 1157  
 Wood, B. E., Müller, H.-R., & Zank, G. P. 2000, *ApJ*, 542, 493  
 Wood, B. E., Müller, H.-R., Zank, G. P., & Linsky, J. L. 2002, *ApJ*, 574, 412 (Paper I)  
 Wood, B. E., Redfield, S., Linsky, J. L., Müller, H.-R., & Zank, G. P. 2005, *ApJS*, 159, 118 (Paper II)  
 Zank, G. P., Pauls, H. L., Williams, L. L., & Hall, D. T. 1996, *J. Geophys. Res.*, 101, 21639